

## Characteristics of superradiant optical phases occurring in the system of nondegenerate $\Lambda$ atoms and radiation that are interacting inside a nonlinear quantum cavity

S. Samimi  and M. M. Golshan \**Physics Department, Science College, Shiraz University, Shiraz 71946-84795, Iran*

(Received 12 October 2021; accepted 19 April 2022; published 3 May 2022)

In the present article, we investigate the behavior of a large collection of three-level  $\Lambda$  atoms interacting with two quantized electromagnetic fields inside a second-order nonlinear quantum cavity. The nonlinearity of the cavity is supposed to be activated by the application of two classical pump fields. The total Hamiltonian of the combination, with due attention to the nonlinearity effects, is diagonalized. The corresponding ground-state energy then follows from minimizing the total Hamiltonian. The structure of the ground state indicates that four distinct optical phases can occur in such a system. These possible phases turn out to be trivial, dark, left-arm and right-arm superradiant ones. Conditions under which any of the four optical phases can actually occur are also analyzed and discussed. The analysis of the conditions, accompanied by several figures, then reveals that with a suitable choice of the pump field amplitudes and/or geometrical phases, one can intensify the two superradiant phases drastically. Moreover, we demonstrate that the dark optical phase cannot occur at all, while the trivial and superradiant ones can, in fact, coexist. Our calculations also show that transition from the trivial phase to left-arm (right-arm) superradiant one is continuous (discrete) and second (first) order in nature. Another important result of our investigation is that by adjusting the pump field strength, one can switch from the left-arm superradiant phase to the right-arm one and vice versa. This point, in turn, provides an alternative mechanism for the development of quantum optical switching devices.

DOI: [10.1103/PhysRevA.105.053702](https://doi.org/10.1103/PhysRevA.105.053702)

### I. INTRODUCTION

The occurrence of superradiation in the system of interacting atoms and quantum electromagnetic fields has been well established by now, both theoretically [1–7] and experimentally [8–11]. In a simple way, such optical phases may be defined as *trivial* (normal) and *superradiant* ones that may exist in a system of a large number of atoms (Dicke states) and quantized electromagnetic fields (photons). Specifically, in the superradiant phase the atoms rise to excited states, and the quantized fields are excited to some combination of non-vanishing occupational states [12–14]. On the other hand, the trivial phase is the case in which all atoms occupy the ground state, while the fields are in the vacuum state [3,14–17]. Physically, the occurrence of nontrivial phases is due to coherent spontaneous atomic radiation [18–20]. In this regard, the question of how such optical phases may be controlled and intensified is still the subject of intensive research projects [21–26]. The control, as well as intensification, of optical phases has been suggested for the development of, among others [27–32], ultrashort coherent light pulse sources [33–36], optical switching devices [37–39], and very low temperature measuring gauges [40,41]. In what follows, we introduce a mechanism to effectively enhance and control the achievable radiant phases. In the proposed mechanism, the atoms are taken as three-level nondegenerate  $\Lambda$  atoms which interact with two quantized fields inside a second-order nonlinear cavity. The nonlinearity of the medium filling the

quantum cavity is induced by externally applying two classical pump fields. As will be demonstrated, the phases and amplitudes of these classical fields provide an efficient mechanism to control the behavior of the atom-field combination.

The notion of controlling the behavior of optical phases in atom-field systems by the application of an externally adjustable agent was discussed in Refs. [25,26]. The most important point in these references is the fact that the external agent stimulates the nonlinearity of the medium which fills the quantum cavity. Moreover, it is by all means possible to control the optical phases intrinsically [42,43]. This, however, can be done only by changing the particular atoms inside the cavity and/or size of the quantum resonator [22,44–46]. In practice, such intrinsic alteration of the system would be of little use. In addition, intrinsic alterations face the more conceptual challenge surrounding the no-go theorem [47]. In the case of either the extrinsic or intrinsic controlling procedure, an attempt is made to break the  $Z_2$  symmetry by adjusting the system's parameters. The latter assessment comes about from the fact that in most systems the total Hamiltonian *conditionally* commutes with the generator of the symmetry ( $U_1$  and/or  $Z_2$ ) [7,48–50]. It is then obvious that by adjusting the system's parameters, one can actually destroy the corresponding symmetry. A survey of the literature reveals that when the atomic system parameters, particularly atomic dipole moments, are specified, the breakage of the symmetry becomes impossible unless a different kind of atom, with some other dipole moments, is used [13,51]. As a result, a transition between optical phases within a *specified* system of atoms and fields is out of the question. In a practical setup, atoms and fields couple in a fixed manner, so that one can make an optical transition only

\*golshan@susc.ac.ir

by changing the atom or cavity parameters. As will be seen, our model overcomes this practical shortcoming.

Even though the study of the system of two- or three-level atoms ( $\Lambda$  and  $V$ ) and radiation fields has filled a textbook [52], the models have been extensively suggested for practical purposes [53–57]. In most treatments, however, atoms and fields interact in an otherwise empty cavity or, at best, one filled with a linear medium. To this end, investigation of the model interacting inside a quantum cavity filled by *nonlinear* media has provided practical methods to manipulate the possible optical phases [25]. Since such a medium may be polarized (which induces polariton waves [26]) by the application of external field pump(s), controlling agents are then at our disposal. It was, moreover, shown that some orders of nonlinearity retain  $Z_2$  symmetry, while other orders lead to its breakage [26]. The more advantageous of these nonlinearity orders (nonlinear susceptibility) is the second-order one. The main aim of the present work is to identify and characterize the optical phases that may turn up in the system of three level  $\Lambda$ -type atoms interacting with two quantum fields inside a second-order nonlinear resonator. The two quantum modes, coupled to the left or right arm of the ( $\Lambda$ ) atoms, then constitute two distinct branches of  $Z_2$  symmetry, which can be broken independently. As demonstrated here, this can happen by adjusting the amplitudes and/or the geometrical phases of the pump fields. To this end, we use the variational principle to determine the system's ground-state energy, per atom, in the thermodynamic limit. As a result, we identify four well-defined optical phases, namely, trivial, dark, “left-arm” (high-frequency) and “right-arm” (low-frequency) superradiant phases. The more important result of the present work is that we explicitly demonstrate the conditions, adjustable by the pump fields, under which the system embraces these phases. Last but not least, the nature of optical phase transitions is also addressed. In fact, it will be shown that a transition between trivial and left-arm superradiant phases is continuous, while that for the right-arm one is discontinuous. The transition from left-arm to right-arm superradiant phases also turns out to be discontinuous.

The organization of this article is as follows. In the next section the model is introduced, and the total Hamiltonian is presented. In Sec. III, we begin by calculating the ground-state energy per atom, in detail. Then two subsections are devoted to the characteristics of left- and right-arm superradiant phases in that order. Following the calculation of the ground-state energies, the conditions for which a possible solution is stable form the subject of Sec. IV. This section also includes figures that adequately describe the behavior and nature of the corresponding optical phases. This article is concluded by highlighting the more important results in Sec. V.

## II. DESCRIPTION OF THE MODEL

The present section is devoted to the description of the model and the corresponding Hamiltonian. The system considered here is formed by a collection of identical  $\Lambda$ -type three-level atoms, interacting with a two-mode radiation field. In addition, it is supposed that the interaction occurs in a quantum cavity filled with nonlinear materials. In order to excite the second-order nonlinearity of the medium in the

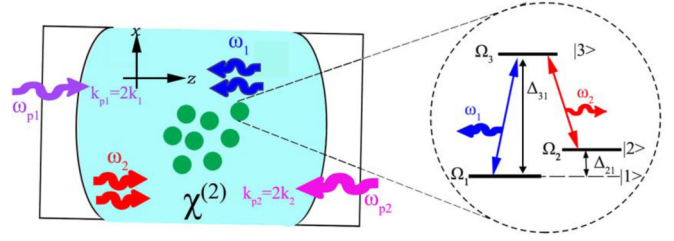


FIG. 1. The nonlinear cavity QED filled by a second-order nonlinear medium.

cavity, two external classical pumps with short duration, with frequency  $\omega_{pi}$  ( $i = 1, 2$ ), are also assumed to be present. These classical fields are responsible for the creation of two quantum fields, characterized by frequencies  $\omega_1$  and  $\omega_2$ . These two fields, in turn, interact with the two arms of the  $\Lambda$ -type atoms. Other characteristics of the system are schematically presented in Fig. 1, which also serves to identify the notations we employ herein. Although Fig. 1 roughly (in the sense that necessary optical elements are omitted; details can be found in Refs. [8,9], for instance) sketches the experimental realization of the system, in the following we present a brief account of the manner with which a second-order nonlinear cavity with embedded  $\Lambda$ -type atoms can be achieved.

In this regard, one may use crystals, in particular, potassium titanyl phosphate (KTP), which exhibit second-order nonlinearity [58–60]. The crystal is then doped with elements belonging to the first column of the periodic table whose ground states are, in fact, degenerate. To this end, the rubidium isotope  $^{87}\text{Rb}$  has been most commonly used, giving the well-known RKTP crystals [61–63]. In order to aggregate the Rb atoms in a very tiny region so that the electric dipole approximation becomes appropriate to employ, one starts the process of doping with a very small (in size) RKTP crystal and a few Rb atoms. The resulting product can then be used as a seed to grow RKTP to a desirable size, in the present case the size of the cavity. As is well known, moreover, Rb atoms (as well as the rest of the group) behave as two levels under ordinary conditions. To remove the degeneracy of the ground state of  $^{87}\text{Rb}$  atoms so that they turn into three-level atoms, the whole (doped) crystal is externally put under the influence of a uniform and static magnetic field. Because of the nonmagnetic properties of the crystal, such a field would solely influence the  $^{87}\text{Rb}$  atoms, giving rise to the separation of the  $|5^2S_{1/2}, F = 1 \text{ or } 2\rangle$  (using spectroscopic notation and the values for  $^{87}\text{Rb}$  total angular momentum, including the nucleus) states that describe the corresponding ground state [64]. Since the amount of energy splitting of the ground-state energy strongly depends upon the magnitude of the external magnetic field, Rb atoms can be realized as  $\Lambda$  atoms with a proper choice of such an external agent.

In accordance with what has been described, the system under consideration is governed by the Hamiltonian

$$\mathcal{H} = \mathcal{H}_f + \mathcal{H}_a + \mathcal{H}_{af} + \mathcal{H}_{ff}. \quad (1)$$

In Eq. (1), the free-field Hamiltonian reads ( $\hbar = 1$  and standard notations)  $\mathcal{H}_f = \sum_{s=1}^2 \omega_s a_s^\dagger a_s$ , and the free atomic

Hamiltonian for a collection of  $N$  identical  $\Lambda$  atoms is

$$\mathcal{H}_a = \sum_{k=1}^3 \Omega_k S_{kk}, \quad S_{kk'} = \sum_{j=1}^N |k\rangle_{jj} \langle k'|. \quad (2)$$

The kets in Eq. (2) describe single atomic states. For future use, we record the following commutation relation for the atomic operators:

$$[S_{kl}, S_{k'l'}] = \delta_{k'l} S_{kl'} - \delta_{kl'} S_{k'l}. \quad (3)$$

Moreover, in the electric dipole and rotating-wave approximations the atom-field interaction  $\mathcal{H}_{af}$  becomes

$$\mathcal{H}_{af} = \frac{\lambda_{13}}{\sqrt{N}} (a_1^\dagger S_{13} + a_1 S_{31}) + \frac{\lambda_{23}}{\sqrt{N}} (a_2^\dagger S_{23} + a_2 S_{32}), \quad (4)$$

where  $\lambda_{13}$  ( $\lambda_{23}$ ) denotes the coupling strength of the left (right) arm of the atom-field interaction. The appearance of  $\sqrt{N}$  in Eq. (4) is due to the fact that the following calculations are carried out in the thermodynamic limit [5,65,66]. It is emphasized that the pump field is way off resonance with atomic states, so it does not participate in the atom-field interaction. As for the field-field interaction, arising from second-order nonlinearity of the cavity, one has [26]  $H_{ff} \sim \int [\sum_\alpha E_\alpha(z, k_\alpha)]^3 dv$ , with the assumption of isotropy and homogeneity of the nonlinear medium filling the cavity. For the case in hand,  $\alpha$  runs over the two quantum-mechanical and two classical fields. For the former ones,  $E_{1,2} \sim [a_{1,2} \exp(ik_{1,2}z) + \text{H.c.}]$ , while for the latter ones (classical fields),  $E_{p_1, p_2} \sim [C_{p_1, p_2} \exp(ik_{p_1, p_2}z + \phi_{p_1, p_2}) + \text{c.c.}]$ , with  $C$  being  $C$  numbers. When expressions for the fields are substituted in  $H_{ff}$  and integration over the volume of the cavity is performed, the results involve cross multiples of field operators and classical  $C$  numbers, each accompanied by  $\delta$  functions. Needless to say, the  $\delta$  functions, whose arguments involve linear combinations of the corresponding wave numbers, arise from the plane-wave nature of the fields. It is then feasible to control the form of  $H_{ff}$  by properly adjusting the wave numbers of the participating fields. Since a cavity of length  $L$  can support modes of wave numbers  $k_i = q_i(\pi/L)$ ,  $i = 1, 2, p_1, p_2$ , where  $q_i$  are integers, we choose the pump fields in such a way that  $k_{p_1} = (q_{p_1}/q_1)k_1$  and  $k_{p_2} = (q_{p_2}/q_2)k_2$ . In this manner, the cavity simultaneously supports all of the fields involved. With this choice of wave numbers, all the terms in  $H_{ff}$  vanish except those composed of  $a_i^{\dagger 2}$  and  $a_i^2$ ,  $i = 1, 2$ . Under these conditions, the field-field interaction then reads [26]

$$\mathcal{H}_{ff} = g_1(E_{p_1}) (a_1^2 e^{i(\omega_{p_1}t + \phi_{p_1})} + a_1^{\dagger 2} e^{-i(\omega_{p_1}t + \phi_{p_1})}) + g_2(E_{p_2}) (a_2^2 e^{i(\omega_{p_2}t + \phi_{p_2})} + a_2^{\dagger 2} e^{-i(\omega_{p_2}t + \phi_{p_2})}), \quad (5)$$

where  $E_{p_i}$  and  $\phi_{p_i}$  ( $i = 1, 2$ ) denote, respectively, the pump amplitude and its initial geometrical phase. As we shall see in Sec. III, right after Eq. (14), the pump phases play a crucial role in determining the nature of superradiant optical phases: solely electric, solely magnetic, and a mixture of the two. Moreover, we define the field-field coupling explicitly as  $g_i = \omega_i \chi^{(2)} E_{p_i}$ , where  $\chi^{(2)}$  denotes the second-order susceptibility of the filling material. The Hilbert space of the system is spanned by the eigenstates of  $\mathcal{H}_f + \mathcal{H}_a$ , which is the tensor product of the two fields states,  $|f_1\rangle$  and  $|f_2\rangle$  (which will

be specified later), and atomic Dicke states,  $|D(j_1, j_2, j_3; N)\rangle$  (indicating that out of  $N$  atoms the  $j_i$  ones are in the  $i$ th state). Following this description of the model, the ground-state energy of the system is determined in the next section.

### III. GROUND-STATE ENERGY OF THE SYSTEM

In order to determine the ground-state energy of the system, we find it more convenient to cast Eq. (1), with due attention to the participating terms, in the Holstein-Primakoff representation [67]. This is done by introducing new atomic (bosonic) operators  $b_{2(3)}$  as

$$S_{ij} = b_i^\dagger b_j \quad i, j \neq 1, \quad (6)$$

$$S_{1i} = S_{11}^{1/2} b_i, \quad S_{i1} = b_i^\dagger S_{11}^{1/2}, \quad (7)$$

and

$$S_{11} = N - b_2^\dagger b_2 - b_3^\dagger b_3. \quad (8)$$

In this equivalent representation,  $b_i$  ( $b_i^\dagger$ ) annihilates (creates) an atom in the  $i$ th state while creating (annihilating) an atom in the atomic ground state. From the commutation relation in Eq. (3), one arrives at  $[b_i^\dagger, b_i] = \delta_{ij}$  and  $[b_i, b_j] = [b_i^\dagger, b_j^\dagger] = 0$ . In the Holstein-Primakoff representation, therefore, the free atomic Hamiltonian becomes

$$\mathcal{H}_a = N\Omega_1 + \Omega_{12} b_2^\dagger b_2 + \Omega_{13} b_3^\dagger b_3, \quad (9)$$

where  $\Omega_{1j} = \Omega_j - \Omega_1$  ( $j = 2, 3$ ). Meanwhile, the atom-field interaction reads

$$\mathcal{H}_{af} = \frac{\lambda_{13}}{\sqrt{N}} (S_{11}^{1/2} a_1^\dagger b_3 + a_1 b_3^\dagger S_{11}^{1/2}) + \frac{\lambda_{23}}{\sqrt{N}} (a_2^\dagger b_2^\dagger b_3 + a_2 b_2 b_3^\dagger). \quad (10)$$

Needless to say, the free-field Hamiltonian and field-field Hamiltonian [Eq. (5)] remain unchanged in this representation. Accordingly, the total Hamiltonian becomes

$$\begin{aligned} \mathcal{H} = & \omega_1 a_1^\dagger a_1 + \omega_2 a_2^\dagger a_2 + N\Omega_1 + \Omega_{12} b_2^\dagger b_2 + \Omega_{13} b_3^\dagger b_3 \\ & + \frac{\lambda_{13}}{\sqrt{N}} (S_{11}^{1/2} a_1^\dagger b_3 + a_1 b_3^\dagger S_{11}^{1/2}) + \frac{\lambda_{23}}{\sqrt{N}} (a_2^\dagger b_2^\dagger b_3 + a_2 b_2 b_3^\dagger) \\ & + g_1(E_{p_1}) (a_1^2 e^{i(\omega_{p_1}t + \phi_{p_1})} + a_1^{\dagger 2} e^{-i(\omega_{p_1}t + \phi_{p_1})}) \\ & + g_2(E_{p_2}) (a_2^2 e^{i(\omega_{p_2}t + \phi_{p_2})} + a_2^{\dagger 2} e^{-i(\omega_{p_2}t + \phi_{p_2})}) \end{aligned} \quad (11)$$

in the Holstein-Primakoff representation. In the next stage, we remove the time dependence of the total Hamiltonian by going to a rotating frame described by the unitary transformation

$$U(t) = \exp[i(\tilde{\omega}_1 a_1^\dagger a_1 + \tilde{\omega}_2 a_2^\dagger a_2 + \tilde{\Omega}_2 b_2^\dagger b_2 + \tilde{\Omega}_3 b_3^\dagger b_3)t]. \quad (12)$$

In this representation, the total Hamiltonian is obtained from  $\tilde{\mathcal{H}} = U\mathcal{H}U^\dagger - iU\frac{\partial U^\dagger}{\partial t}$ , whose result involves time-dependent exponentials. To get rid of the time dependence, one sets the exponents equal to zero, which provides a set of equations for  $\tilde{\omega}$  and  $\tilde{\Omega}$  in terms of  $\omega_p$ . As the solutions to the set of such equations, it is found that  $\tilde{\omega}_i = \omega_{p_i}/2$ ,  $\tilde{\Omega}_2 = (\omega_{p_1} - \omega_{p_2})/2$ , and  $\tilde{\Omega}_3 = \omega_{p_1}/2$ , which indeed do the job. Adopting these expressions for the frequencies, the total Hamiltonian turns

out to be

$$\begin{aligned} \tilde{\mathcal{H}} = & \delta_1 a_1^\dagger a_1 + \delta_2 a_2^\dagger a_2 + N\Omega_1 + \Delta_2 b_2^\dagger b_2 + \Delta_3 b_3^\dagger b_3 \\ & + \frac{\lambda_{13}}{\sqrt{N}} (S_{11}^{1/2} a_1^\dagger b_3 + a_1 b_3^\dagger S_{11}^{1/2}) + \frac{\lambda_{23}}{\sqrt{N}} (a_2^\dagger b_2^\dagger b_3 + a_2 b_2 b_3^\dagger) \\ & + g_1 (a_1^2 e^{i\phi_{p1}} + a_1^{\dagger 2} e^{-i\phi_{p1}}) + g_2 (a_2^2 e^{i\phi_{p2}} + a_2^{\dagger 2} e^{-i\phi_{p2}}) \end{aligned} \quad (13)$$

in the rotating frame. The new field and atomic frequencies are now defined as  $\delta_s = \omega_s - \tilde{\omega}_s$  ( $s = 1, 2$ ) and  $\Delta_i = \Omega_{1i} - \tilde{\Omega}_i$  ( $i = 2, 3$ ), respectively. We are now in a position to calculate the system's ground-state energy in the limit of a large atomic number. It is well known [68,69] that in this limit the field ground state  $|G\rangle$  approaches a coherent state,  $|f_i\rangle \rightarrow |\sqrt{N}\alpha_i\rangle$ , while the atoms also fall into a coherent state,  $|D(j_1, j_2, j_3; N)\rangle \rightarrow |\sqrt{N}\beta_2, \beta_3\rangle$ . The ground state then reads  $|\sqrt{N}\alpha_1\rangle \otimes |\sqrt{N}\alpha_2\rangle \otimes |\sqrt{N}\beta_2\rangle \otimes |\sqrt{N}\beta_3\rangle$  in this limit. Here  $|\sqrt{N}\alpha_i\rangle$  ( $|\sqrt{N}\beta_i\rangle$ ) denotes the photonic (atomic) coherent states. The inclusion of  $\sqrt{N}$  guarantees that the ground-state energy per atom,  $h_G = \langle G|\tilde{\mathcal{H}}|G\rangle/N$ , remains constant in the thermodynamic limit. To find the ground-state energy per atom, we take  $\alpha$  and  $\beta$  as variational parameters and minimize  $h_G$ . To this end, we find

$$\begin{aligned} h_G = & \Omega_1 + \delta_1 \alpha_1^2 + \delta_2 \alpha_2^2 + \Delta_2 \beta_2^2 + \Delta_3 \beta_3^2 - 2g_1 \alpha_1^2 - 2g_2 \alpha_2^2 \\ & + 2\lambda_{13} \sqrt{1 - \beta_2^2 - \beta_3^2} \alpha_1 \beta_3 + 2\lambda_{23} \alpha_2 \beta_2 \beta_3, \end{aligned} \quad (14)$$

where we have taken pump-field initial phases as  $\pi$  and, at the same time, the variational parameters to be real. From the definition  $\alpha_i \pm \alpha_i^*$  for the photonic quadrature, the associated magnetic field is absent following these choices. Although the following calculation may be readily extended to the case of a solely magnetic phase (taking the initial geometric phase as  $\pi/2$ ) or a mixture of electric and magnetic phases (taking any value for the geometrical phase other than 0,  $\pi$  or  $\pi/2$ ), the conclusions we shall draw apply. It is noted that  $h_G$ , being the expectation value of a Hermitian operator, must be real valued. This fact implies that  $\beta_2^2 + \beta_3^2 \leq 1$ , meaning that physically, the population of states  $|2\rangle$  and  $|3\rangle$  cannot exceed the total number of atoms. The equality sign indicates the border of regions in which differentiation with respect to  $\beta_2$  and  $\beta_3$  is not defined. Equating differentials of  $h_G$  with respect to  $\alpha_1$  and  $\alpha_2$  separately to zero and solving the resulting two equations gives

$$\alpha_1 = \frac{\beta_3 \lambda_{13} \sqrt{1 - \beta_2^2 - \beta_3^2}}{2g_1 - \delta_1} \quad (15)$$

and

$$\alpha_2 = \frac{\lambda_{23} \beta_2 \beta_3}{2g_2 - \delta_2}. \quad (16)$$

The following sections are devoted to an investigation of the conditions under which left-arm and right-arm superradiation modes appear.

### A. Left-arm superradiance phase

When Eqs. (15) and (16) are substituted into  $h_G$  and the result of differentiation (it is implicitly assumed that

$\beta_2^2 + \beta_3^2 < 1$ ) with respect to  $\beta_2$  is set to zero, one finds

$$\begin{aligned} & \left( g_1 \lambda_{23}^2 - g_2 \lambda_{13}^2 - \frac{\delta_1 \lambda_{23}^2}{2} + \frac{\delta_2 \lambda_{13}^2}{2} \right) \beta_3^2 \beta_2 \\ & - (2g_1 - \delta_1)(2g_2 - \delta_2) \Delta_2 \beta_2 = 0. \end{aligned} \quad (17)$$

The solution to Eq. (17) is, evidently, either  $\beta_2 = 0$  when  $\beta_3$  is undetermined (which will be found momentarily) or  $\beta_2 \neq 0$  and  $\beta_3 = \pm \sqrt{\Delta_2 \left( \frac{\lambda_{13}^2}{2g_1 - \delta_1} - \frac{\lambda_{23}^2}{2g_2 - \delta_2} \right)^{-\frac{1}{2}}$  for points inside the circle  $\beta_2^2 + \beta_3^2 = 1$ . Moreover, plugging  $\beta_2 = 0$  into Eq. (16) gives  $\alpha_2 = 0$ , indicating that the right-arm radiation is in the trivial phase, while the behavior of the left-arm radiation is yet undetermined. However, for the latter set of solutions, one can straightforwardly calculate the Hessian matrix and conclude that for these solutions the behavior of the system is *not* stable. Disregarding these solutions, we substitute  $\beta_2 = 0$  into Eq. (15) and plug the result, along with the fact that  $\alpha_2 = 0$ , into Eq. (14), giving

$$h_G^L = -\frac{\lambda_{13}^2}{2g_1 - \delta_1} \beta_3^4 + \left( \Delta_3 + \frac{\lambda_{13}^2}{2g_1 - \delta_1} \right) \beta_3^2 + \Omega_1, \quad (18)$$

which upon minimization leads to the equation

$$\frac{dh_G^L}{d\beta_3} = -\frac{4\lambda_{13}^2}{2g_1 - \delta_1} \beta_3^3 + 2 \left( \Delta_3 + \frac{\lambda_{13}^2}{2g_1 - \delta_1} \right) \beta_3 = 0 \quad (19)$$

for the determination of  $\beta_3$ . The solution to Eq. (19) is

$$\beta_3 = 0 \quad \text{or} \quad \beta_3 = \pm \left( \frac{x - x_c}{1 - 2x_c} \right)^{\frac{1}{2}}, \quad (20)$$

where  $x = g_1/\delta_1$  and  $x_c = 1/2[1 - \lambda_{13}^2/(\Delta_3 \delta_1)] \leq 1/2$ . The system's trivial optical phase corresponds to  $\beta_3 = 0$ , for which  $\alpha_1 = \alpha_2 = \beta_2 = 0$  [see Eqs. (15) and (16)]. The trivial optical phase, as seen from Eq. (18), has an energy of  $\Omega_1$ , a physically reasonable result. On the other hand,  $\beta_3 \neq 0$  conditionally gives rise to the left-arm superradiant optical phase. It is worth noting that the nontrivial solution for  $\beta_3$  never diverges because  $\lambda_{13}$  cannot vanish for the system under consideration. Moreover, the assumption that  $\beta_3$  is a real number restricts the values of  $x (= g_1/\delta_1)$  to the inequality  $x_c \leq x < 1/2$ . From the second derivative of Eq. (18), it is readily concluded that if the aforementioned inequality is not satisfied, the trivial solution is stable, while the superradiant one becomes unstable and vice versa. Using the nontrivial solution for the left-arm superradiant phase, i.e.,  $\alpha_2 = \beta_2 = 0$  and  $\beta_3$  as in Eq. (20), in Eq. (16), one finds

$$\alpha_1 = \mp \frac{\sqrt{\Delta_3/\delta_1} \left[ \frac{(1-2x) + (x-x_c)}{1-2x_c} (x-x_c) \right]^{\frac{1}{2}}}{1-2x}, \quad (21)$$

which is also real since the condition  $x_c \leq x < 1/2$  has been assumed to hold. For completeness and use in the next section the nontrivial solution for  $\beta_3$  [see Eq. (20)] is substituted into Eq. (18) to obtain the left-arm superradiant total energy per atom as

$$(h_G^L)_s = \Omega_1 - \frac{\Delta_3}{(1-2x_c)(1-2x)} (x-x_c)^2. \quad (22)$$

It is also worth noting that if  $\Delta_3 (= \Omega_{13} - \Omega_{p1}/2) = 0$ , one has  $\alpha_1 = \alpha_2 = \beta_2 = 0$ , while  $\beta_3 \neq 0$  [see Eq. (20)], which

corresponds to the left-arm dark state, also with an energy  $\Omega_1$ . Note that the condition  $\Delta_3 = 0$  can be achieved through the adjustment of the first pump-field frequency. From the definition of  $x_c$  [see the text after Eq. (20)], we conclude that it approaches  $-\infty$  when  $\Delta_3 = 0$ , for which the condition  $x > x_c$  always holds. In this limit,  $(\beta_3^L)_D \rightarrow \pm 1/\sqrt{2}$ , meaning that in the left-arm dark state the population is half in level |1> and half in level |3>. As a final point, we state that the dark phase is not stable unless  $\Delta_3$  vanishes. In the latter case the trivial and dark phases become degenerate.

### B. Right-arm superradiance phase

Since a transition of the type  $|1\rangle \leftrightarrow |2\rangle$  is forbidden in the model under consideration, it is expected that the right-arm superradiant phase is possible only when  $\beta_2^2 + \beta_3^2 = 1$ , indicating that all atoms are distributed among states |2> and |3>. Using the constraint  $\beta_2^2 + \beta_3^2 = 1$  in Eq. (15) gives  $\alpha_1 = 0$ . Then from Eq. (14), along with Eq. (16), the right-arm energy per atom is

$$h_G^R = \frac{-\lambda_{23}^2}{2g_2 - \delta_2} \beta_3^4 + \left( \Delta_3 - \Delta_2 + \frac{\lambda_{23}^2}{2g_2 - \delta_2} \right) \beta_3^2 + \Delta_2 + \Omega_1. \quad (23)$$

Again, we differentiate Eq. (23) with respect to  $\beta_3$  and equate the result to zero, giving either  $\beta_3 = 0$  or

$$(\beta_3^R)_s = \pm \left[ \frac{(1 - y - y_c)\sqrt{\Delta_2} + (y - y_c)\sqrt{\Delta_3}}{(\sqrt{\Delta_2} + \sqrt{\Delta_3})(1 - 2y_c)} \right]^{\frac{1}{2}}, \quad (24)$$

where  $y = g_2/\delta_2$  and  $y_c$  is defined as

$$y_c = \frac{1}{2} \left[ 1 - \frac{\lambda_{23}^2}{\delta_2(\sqrt{\Delta_2} + \sqrt{\Delta_3})^2} \right]. \quad (25)$$

Here again,  $(\beta_3^R)_s$  is a finite parameter since  $y_c < 1/2$  unless  $\lambda_{23} = 0$ , which is impossible. As in the case of left-arm superradiance, the positiveness of the second derivative of Eq. (23) is guaranteed if and only if  $y_c < y < 1/2$  is satisfied. Needless to say, the latter condition also guarantees the reality of  $(\beta_3^R)_s$ . To further specify the characteristics of the right-arm superradiant phase,  $(\beta_3^R)_s$  in Eq. (24), along with the constraint, is used in Eq. (16), leading to

$$(\alpha_2^R)_s = \mp \frac{[(1 - y - y_c)\sqrt{\Delta_3} + (y - y_c)\sqrt{\Delta_2}]^{1/2}}{(1 - 2y)[(1 - 2y)\delta_2]^{1/2}} \times [(1 - y - y_c)\sqrt{\Delta_2} + (y - y_c)\sqrt{\Delta_3}]^{1/2}, \quad (26)$$

which, in turn, gives the number of photons in the second radiation mode. The right-arm superradiant phase drastically differs from the left-arm superradiant phase since some of the atoms still occupy the middle level. In fact, when the expression for  $(\beta_3^R)_s$  is used in the constraint  $\beta_2^2 + \beta_3^2 = 1$ , the result is

$$(\beta_2^R)_s = \pm \left[ \frac{(1 - y - y_c)\sqrt{\Delta_3} + (y - y_c)\sqrt{\Delta_2}}{(\sqrt{\Delta_3} + \sqrt{\Delta_2})(1 - 2y_c)} \right]^{1/2}. \quad (27)$$

If Eq. (24) is substituted into Eq. (23), one obtains

$$(h_G^R)_s = \Omega_1 + \Delta_2 - \frac{[(1 - y - y_c)\sqrt{\Delta_2} + (y - y_c)\sqrt{\Delta_3}]^2}{(1 - 2y)(1 - 2y_c)} \quad (28)$$

for the ground-state energy per atom of the right-arm superradiant phase. Moreover, when  $\beta_3 = 0$  is plugged into  $\beta_2^2 + \beta_3^2 = 1$ , one finds  $\beta_2 = \pm 1$ , which indicates that all atoms occupy the middle level. Plugging the value for  $\beta_3$  in Eqs. (15) and (16),  $\alpha_1 = 0$  and  $\alpha_2 = 0$  result. These four values correspond to the so-called dark state of the system. In the right-arm dark state, the total energy per atom is readily seen from Eq. (23) to be  $(h_G^R)_D = \Omega_1 + \Delta_2$ . Having described the four possible optical phases that may occur in the system of  $\Lambda$  atoms interacting with two photonic modes, two fundamental questions still remain. First, one has to determine which one of the four phases possesses the least energy since the system falls in the corresponding phase when equilibrium is achieved. Second, the nature of such a phase transition also needs to be specified. The next section is thus devoted to a discussion of these two points.

## IV. OPTICAL PHASES: STABILITY AND NATURE OF TRANSITIONS

So far, the conditions under which the second derivative of the energy per atom for both the left-arm and right-arm cases [Eqs. (18) and (23), respectively] is positive have been demonstrated. Now we have to determine which of the four ground-state energies per atom, corresponding to the possible optical phases, forms the absolute minimum. Since the energies of trivial and dark-state phases are constant, in what follows, our attention is focused on examining the two superradiant phases. To this end, we equate the corresponding ground-state energies of the two modes, Eqs. (22) and (28), and solve for  $y$  in terms of  $x$ ,  $y = y(x)$ . Recalling the discussion presented in the previous section, the graph  $y = y(x)$ , along with  $x = x_c$  and  $y_c = y(x_c)$ , specifies the borders of the regions inside which different phases occur. Although the expression for  $y = y(x)$  is readily available, it is so involved that we cannot present its form here. Putting all these together, one can generate the phase diagram in Fig. 2, where the regions corresponding to the left-arm [blue (dark gray) area] and right-arm [red (light gray) area] superradiant phases and the trivial phase (white area) are vividly specified. It should be pointed out that each region in Fig. 2 specifies the conditions for which the corresponding energy forms an absolute minimum. We remind ourselves of the important point that the blue (dark gray) region as well as the white one can happen only for points *inside* the bordering circle,  $\beta_2^2 + \beta_3^2 = 1$ . For points *on* the border line only the red (light gray) region appears. Moreover, it is noted that in Fig. 2, no region for the dark states appears. This point comes about from the fact that dark-state energies  $(h_G^{L(R)})_D$  are larger than that of the trivial-phase energy, unless the detunings vanish. In that case the dark states become degenerate with the trivial phase and fall into the white area. For conciseness, we just state from Fig. 2 that with an appropriate choices of  $x = g_1(E_{p1})/\delta_1$  and  $y = g_2(E_{p2})/\delta_2$ , through the amplitude of the pump fields, one can force the system to fall into any of the optical phases.

Another interesting point drawn from Fig. 2 is the fact that in the present system a so-called triple (tricritical) point does exist. This corresponds to the intersection of  $x_c$ ,  $y_c$ , and  $y(x)$ , indicating that all the optical phases coexist at this point. For completeness, in Fig. 2 we use the solid curve and

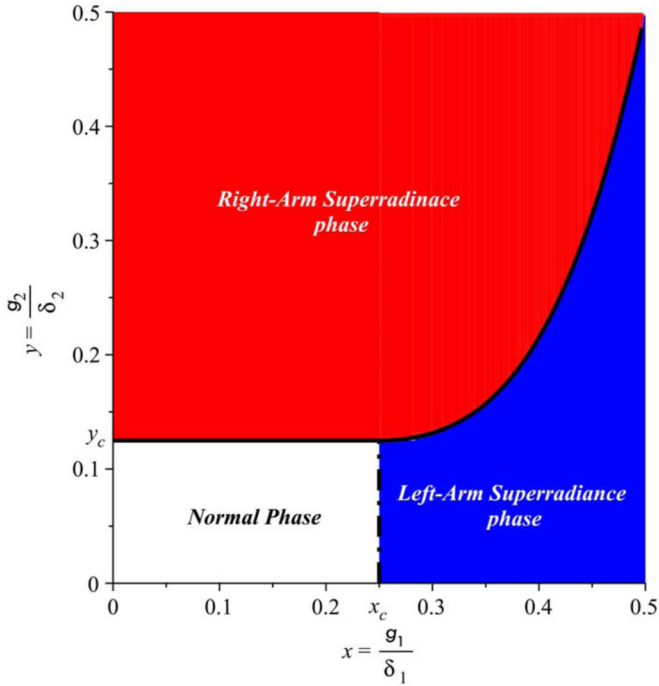


FIG. 2. The system's phase diagram for parameters  $\frac{\Delta_2}{\Delta_3} = 0.5$ ,  $\frac{\delta_1}{\Delta_3} = 0.25$ ,  $\frac{\delta_2}{\Delta_3} = 0.5$ ,  $y_c = 0.125$ , and  $x_c = 0.25$ . Here, the solid curve shows a first-order phase transition, while the dot-dashed line indicates a second-order phase transition.

dashed-dotted line for first-order (discrete) and second-order (continuous) phase transitions, respectively. A full discussion of the nature of such transitions follows momentarily.

The first clue about the nature of optical phase transitions comes from a glance at Fig. 3, where  $\beta_3^2$  versus  $x$  and  $y$  [extracted from Eqs. (20) and (24)] is depicted. Again, Fig. 3 is generated for points inside or on the border of the circle. The main reason for choosing  $\beta_3^2$ , which measures the population

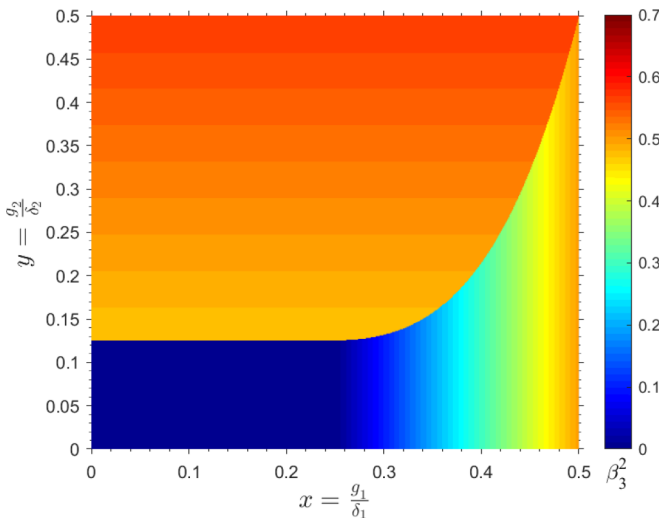


FIG. 3. Population of the atomic  $|3\rangle$  state ( $\sim \beta_3^2$ ) versus  $x = g_1/\delta_1$  and  $y = g_2/\delta_2$ . The system parameters used here are the same as those in Fig. 2.

of state  $|3\rangle$ , is the fact that left-arm (or right-arm) radiation in our system mostly depends upon this population. Observation of the color spectrum (especially the color bar) clearly reveals that the transition from the left-arm superradiant phase (or the trivial one) to right-arm superradiation is discontinuous and of first order. On the other hand, the transition from the trivial phase to the left-arm superradiant one is continuous and of second order. The consistency of Figs. 2 and 3 must be emphasized. From the meaning of  $\beta_3^2$  and the observation of Fig. 3, it is also concluded that for  $x \approx 0.5$  and any  $y$ ,  $\beta_3^2$  is very large, indicating that the left-arm radiation intensity is also very large. The right-arm superradiance is most intense for  $y$  near 0.5 regardless of  $x$ .

To extract more information about the characteristics of the system's superradiant phases, left-arm and right-arm photon numbers, proportional to  $(\alpha_1)^2$  and  $(\alpha_2)^2$ , respectively, are illustrated in Figs. 4(a) and 4(b). The independent variables in these two parts are  $g_1 [= g_1(E_{p1})]$  and  $g_2 [= g_2(E_{p2})]$ , respectively. As the insets indicate, the curves are generated for values of the other pump field under or above the corresponding critical points. For comparison, in both parts the counterpart photon number is also depicted by red solid lines for  $g_2 = 0.15\delta_2$  in Fig. 4(a) and  $g_1 = 0.35\delta_1$  in Fig. 4(b). Figure 4(a) clearly exhibits a phase transition from the trivial phase to left-arm superradiant one continuously, in complete agreement with our earlier conclusion on the subject. Moreover, as the first pump strength passes the corresponding critical points,  $(\alpha_1)^2$  drastically increases. Since such values of  $g_1$  simultaneously throw most atoms in the  $|3\rangle$  state (see Fig. 4), one can achieve an extraordinary superradiant phase. Conclusions of this sort can also be drawn from Fig. 4(b) to generate the right-arm characteristics, again showing the possibility of achieving an extraordinary superradiant phase. The only difference is the nature of the phase transition in this case is discontinuous. Moreover, a comparison of the behavior of  $(\alpha_2)^2$  (red solid curve) with that of  $(\alpha_1)^2$  in Fig. 4(a) reveals an important result: By controlling the pump fields, one can *switch* from the right-arm superradiant phase to the left-arm superradiant phase and vice versa. As a concrete example, Fig. 4(a) shows that for  $g_1$  less than  $\approx 0.34\delta_1$  only the right-arm superradiant phase occurs, while when  $g_1$  passes this value, solely the left-arm field becomes activated.

## V. CONCLUSION

The present work concerns a detailed examination of the optical phases that occur in a large collection of three-level nondegenerate  $\Lambda$ -type atoms, interacting with two quantized fields, inside a perfect cavity. The quantum cavity is filled with a second-order optically nonlinear medium, which is activated by two classical pump fields. It was, moreover, assumed that each quantum field interacts with either the left arm or right arm of the  $\Lambda$ -type atoms. To proceed, we calculated the system's ground-state energy, thereby showing that the  $Z_2$  symmetry inherited by the system only conditionally holds. We further determined the critical values, controllable by the pump fields, for which the  $Z_2$  symmetry ceases to hold. An examination of these values then revealed that four distinct optical phases can exist in such a system. These four possible optical phases are trivial, dark, left-arm, and right-

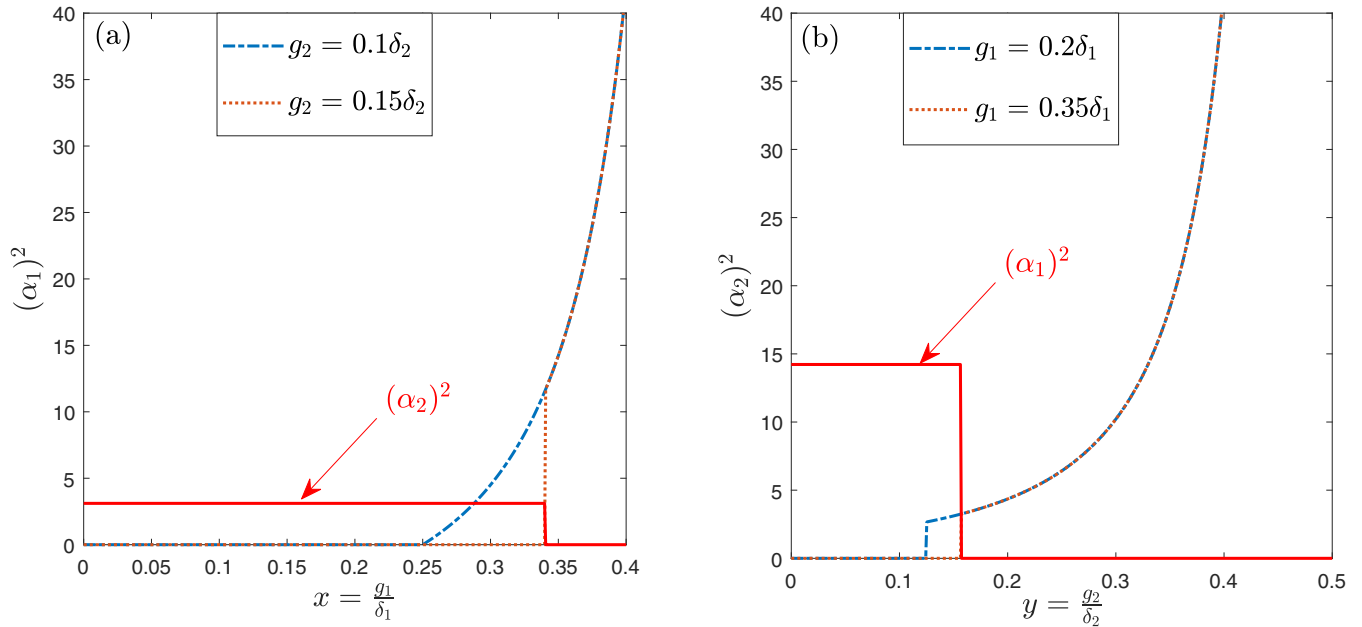


FIG. 4. Behavior of (a) the left-arm and (b) right-arm photonic number versus  $g_1(E_{p1})$  and  $g_2(E_{p2})$ , respectively. The system parameters are the same as those used in the previous figures.

arm superradiant phases. Along these lines, moreover, the characteristics of each optical phase were also deduced and discussed. Moreover, a full discussion of the stability of the four optical phases when the conditions for their occurrence are satisfied was presented. To this end, we demonstrated that when they occur, the dark phase is not stable, while the trivial one indeed is [see also the discussion following Eqs. (22) and (28) and Fig. 2]. On the other hand, when the pump fields are set in such a way that either the left-arm or right-arm superradiant mode is triggered, the resulting phase becomes stable (see the discussion surrounding Fig. 3). Another point of interest that we demonstrated in the present work is the manner by which one can cause the transition between the left-arm and right-arm superradiant modes at will simply by adjusting the amplitudes of the pumping agents. Last but not least, an important result of our investigation is the specification of the nature of the transition between the aforementioned optical phases. As we have fully discussed, the transition from

the trivial phase to the left-arm superradiant phase is continuous and of second order. On the other hand, the transition from the left-arm superradiant phase (or trivial phase) to the right-arm one is discrete and first order in nature (see Figs. 3 and 4).

In view of the above points, the material presented in this article sheds light on the nature and characteristics of optical phases occurring in the system of three-level  $\Lambda$  atoms and two quantized fields. The finer points of the present article may indeed pave the way to the development of means to effectively control the optical phases and thus a novel switching mechanism.

#### ACKNOWLEDGMENT

This work was, in part, supported by a grant from the Research Council of Shiraz University under Contract No. 99GRD1M1110.

- [1] K. Hepp and E. H. Lieb, On the superradiant phase transition for molecules in a quantized radiation field: The Dicke maser model, *Ann. Phys. (NY)* **76**, 360 (1973).
- [2] H.-P. Eckle and H. Johansson, A generalization of the quantum Rabi model: Exact solution and spectral structure, *J. Phys. A* **50**, 294004 (2017).
- [3] M.-J. Hwang, P. Rabl, and M. B. Plenio, Dissipative phase transition in the open quantum Rabi model, *Phys. Rev. A* **97**, 013825 (2018).
- [4] D. Guerzi, P. Simon, and C. Mora, Superradiant Phase Transition in Electronic Systems and Emergent Topological Phases, *Phys. Rev. Lett.* **125**, 257604 (2020).
- [5] D. S. Shapiro, W. V. Pogosov, and Y. E. Lozovik, Universal fluctuations and squeezing in a generalized Dicke model near

the superradiant phase transition, *Phys. Rev. A* **102**, 023703 (2020).

- [6] Y. Lei and S. Zhang, Superradiant phase transition with cavity-assisted dynamical spin-orbit coupling, *Phys. Rev. A* **103**, 053318 (2021).
- [7] R. Palacino and J. Keeling, Atom-only theories for  $U(1)$  symmetric cavity-QED models, *Phys. Rev. Research* **3**, L032016 (2021).
- [8] X. Zhang, Y. Chen, Z. Wu, J. Wang, J. Fan, S. Deng, and H. Wu, Observation of a superradiant quantum phase transition in an intracavity degenerate Fermi gas, *Science* **373**, 1359 (2021).
- [9] M.-L. Cai, Z.-D. Liu, W.-D. Zhao, Y.-K. Wu, Q.-X. Mei, Y. Jiang, L. He, X. Zhang, Z.-C. Zhou, and L.-M. Duan, Observation of a quantum phase transition in the quantum Rabi

- model with a single trapped ion, *Nat. Commun.* **12**, 1126 (2021).
- [10] P. Solano, P. Barberis-Blostein, F. K. Fatemi, L. A. Orozco, and S. L. Rolston, Super-radiance reveals infinite-range dipole interactions through a nanofiber, *Nat. Commun.* **8**, 1857 (2017).
- [11] S. J. Roof, K. J. Kemp, M. D. Havey, and I. M. Sokolov, Observation of Single-Photon Superradiance and the Cooperative Lamb Shift in an Extended Sample of Cold Atoms, *Phys. Rev. Lett.* **117**, 073003 (2016).
- [12] J. Peng, E. Rico, J. Zhong, E. Solano, and I. L. Egusquiza, Unified superradiant phase transitions, *Phys. Rev. A* **100**, 063820 (2019).
- [13] L. Garbe, I. L. Egusquiza, E. Solano, C. Ciuti, T. Coudreau, P. Milman, and S. Felicetti, Superradiant phase transition in the ultrastrong-coupling regime of the two-photon Dicke model, *Phys. Rev. A* **95**, 053854 (2017).
- [14] J. Larson and E. K. Irish, Some remarks on superradiant-phase transitions in light-matter systems, *J. Phys. A* **50**, 174002 (2017).
- [15] K. Baumann, R. Mottl, F. Brennecke, and T. Esslinger, Exploring Symmetry Breaking at the Dicke Quantum Phase Transition, *Phys. Rev. Lett.* **107**, 140402 (2011).
- [16] M.-J. Hwang and M. B. Plenio, Quantum Phase Transition in the Finite Jaynes-Cummings Lattice Systems, *Phys. Rev. Lett.* **117**, 123602 (2016).
- [17] K. Baumann, C. Guerlin, F. Brennecke, and T. Esslinger, Dicke quantum phase transition with a superfluid gas in an optical cavity, *Nature (London)* **464**, 1301 (2010).
- [18] R. H. Dicke, Coherence in spontaneous radiation processes, *Phys. Rev.* **93**, 99 (1954).
- [19] Y. K. Wang and F. Hioe, Phase transition in the Dicke model of superradiance, *Phys. Rev. A* **7**, 831 (1973).
- [20] A. V. Andreev, V. I. Emel'yanov, and Yu. A. Il'inskiĭ, Collective spontaneous emission (Dicke superradiance), *Sov. Phys. Usp.* **23**, 493 (1980).
- [21] W. Kopylov, C. Emary, E. Schll, and T. Brandes, Time-delayed feedback control of the Dicke-Hepp-Lieb superradiant quantum phase transition, *New J. Phys.* **17**, 013040 (2015).
- [22] A. Baksic and C. Ciuti, Controlling Discrete and Continuous Symmetries in "Superradiant" Phase Transitions with Circuit QED Systems, *Phys. Rev. Lett.* **112**, 173601 (2014).
- [23] P. Kirton and J. Keeling, Superradiant and lasing states in driven-dissipative Dicke models, *New J. Phys.* **20**, 015009 (2018).
- [24] A. Patra, B. L. Altshuler, and E. A. Yuzbashyan, Driven-dissipative dynamics of atomic ensembles in a resonant cavity: Nonequilibrium phase diagram and periodically modulated superradiance, *Phys. Rev. A* **99**, 033802 (2019).
- [25] C. J. Zhu, L. L. Ping, Y. P. Yang, and G. S. Agarwal, Squeezed Light Induced Symmetry Breaking Superradiant Phase Transition, *Phys. Rev. Lett.* **124**, 073602 (2020).
- [26] S. Samimi and M. M. Golshan, Switchability of multimodal optical phases in a leaky and nonlinear quantum cavity, *Phys. Rev. A* **103**, 033712 (2021).
- [27] L. Garbe, M. Bina, A. Keller, M. G. A. Paris, and S. Felicetti, Critical Quantum Metrology with a Finite-Component Quantum Phase Transition, *Phys. Rev. Lett.* **124**, 120504 (2020).
- [28] P. P. Vasil'ev, R. V. Penty, and I. H. White, Pulse generation with ultra-superluminal pulse propagation in semiconductor heterostructures by superradiant-phase transition enhanced by transient coherent population gratings, *Light Sci. Appl.* **5**, e16086 (2016).
- [29] P. Zanardi, M. G. A. Paris, and L. Campos Venuti, Quantum criticality as a resource for quantum estimation, *Phys. Rev. A* **78**, 042105 (2008).
- [30] P. A. Ivanov and D. Porras, Adiabatic quantum metrology with strongly correlated quantum optical systems, *Phys. Rev. A* **88**, 023803 (2013).
- [31] M. Tsang, Quantum transition-edge detectors, *Phys. Rev. A* **88**, 021801(R) (2013).
- [32] S. Fernández-Lorenzo and D. Porras, Quantum sensing close to a dissipative phase transition: Symmetry breaking and criticality as metrological resources, *Phys. Rev. A* **96**, 013817 (2017).
- [33] J. G. Bohnet, Z. Chen, J. M. Weiner, D. Meiser, M. J. Holland, and J. K. Thompson, A steady-state superradiant laser with less than one intracavity photon, *Nature (London)* **484**, 78 (2012).
- [34] V. V. Kocharovskiy, V. V. Zheleznyakov, E. R. Kocharovskaya, and V. V. Kocharovskiy, Superradiance: The principles of generation and implementation in lasers, *Phys. Usp.* **60**, 345 (2017).
- [35] H. Liu, S. B. Jäger, X. Yu, S. Touzard, A. Shankar, M. J. Holland, and T. L. Nicholson, Rugged MHz-Linewidth Superradiant Laser Driven by a Hot Atomic Beam, *Phys. Rev. Lett.* **125**, 253602 (2020).
- [36] J. Vieira, M. Pardal, J. Mendonça, and R. Fonseca, Generalized superradiance for producing broadband coherent radiation with transversely modulated arbitrarily diluted bunches, *Nat. Phys.* **17**, 99 (2021).
- [37] D. Ferrari, G. Celardo, G. P. Berman, R. Sayre, and F. Borgonovi, Quantum biological switch based on superradiance transitions, *J. Phys. Chem. C* **118**, 20 (2014).
- [38] Z. Wang, H. Li, W. Feng, X. Song, C. Song, W. Liu, Q. Guo, X. Zhang, H. Dong, D. Zheng, H. Wang, and D.-W. Wang, Controllable Switching between Superradiant and Subradiant States in a 10-Qubit Superconducting Circuit, *Phys. Rev. Lett.* **124**, 013601 (2020).
- [39] K. C. Stitely, S. J. Masson, A. Giraldo, B. Krauskopf, and S. Parkins, Superradiant switching, quantum hysteresis, and oscillations in a generalized Dicke model, *Phys. Rev. A* **102**, 063702 (2020).
- [40] C.-Y. Chen, I.-W. Un, N.-H. Tai, and T.-J. Yen, Asymmetric coupling between subradiant and superradiant plasmonic resonances and its enhanced sensing performance, *Opt. Express* **17**, 15372 (2009).
- [41] A. Y. Bazhenov, D. Tsarev, and A. Alodjants, Temperature quantum sensor on superradiant phase-transition, *Phys. B (Amsterdam, Neth.)* **579**, 411879 (2020).
- [42] N. Lambert, C. Emary, and T. Brandes, Entanglement and the Phase Transition in Single-Mode Superradiance, *Phys. Rev. Lett.* **92**, 073602 (2004).
- [43] S. Ashhab, Superradiance transition in a system with a single qubit and a single oscillator, *Phys. Rev. A* **87**, 013826 (2013).
- [44] Y. Zhang, B.-B. Mao, D. Xu, Y.-Y. Zhang, W.-L. You, M. Liu, and H.-G. Luo, Quantum phase transitions and critical behaviors in the two-mode three-level quantum Rabi model, *J. Phys. A* **53**, 315302 (2020).

- [45] X.-Y. Chen, Y.-F. Xie, and Q.-H. Chen, Quantum criticality of the Rabi-Stark model at finite frequency ratios, *Phys. Rev. A* **102**, 063721 (2020).
- [46] B.-B. Mao, L. Li, W.-L. You, and M. Liu, Superradiant phase transition in quantum Rabi dimer with staggered couplings, *Phys. A (Amsterdam, Neth.)* **564**, 125534 (2021).
- [47] P. Nataf and C. Ciuti, No-go theorem for superradiant quantum phase transitions in cavity QED and counter-example in circuit QED, *Nat. Commun.* **1**, 72 (2010).
- [48] J. Ye and C.-L. Zhang, Superradiance, Berry phase, photon phase diffusion, and number squeezed state in the U(1) Dicke (Tavis-Cummings) model, *Phys. Rev. A* **84**, 023840 (2011).
- [49] M. Soriente, T. L. Heugel, K. Omiya, R. Chitra, and O. Zilberberg, Distinctive class of dissipation-induced phase transitions and their universal characteristics, *Phys. Rev. Research* **3**, 023100 (2021).
- [50] D. Braak, Integrability of the Rabi Model, *Phys. Rev. Lett.* **107**, 100401 (2011).
- [51] L. Garbe, P. Wade, F. Minganti, N. Shammah, S. Felicetti, and F. Nori, Dissipation-induced bistability in the two-photon Dicke model, *Sci. Rep.* **10**, 13408 (2020).
- [52] A. B. Klimov and S. M. Chumakov, *A Group-Theoretical Approach to Quantum Optics: Models of Atom-Field Interactions* (Wiley, Hoboken, NJ, 2009).
- [53] M. Hayn, C. Emary, and T. Brandes, Phase transitions and dark-state physics in two-color superradiance, *Phys. Rev. A* **84**, 053856 (2011).
- [54] M. Hayn, C. Emary, and T. Brandes, Superradiant phase transition in a model of three-level- $\lambda$  systems interacting with two bosonic modes, *Phys. Rev. A* **86**, 063822 (2012).
- [55] A. Baksic, P. Nataf, and C. Ciuti, Superradiant phase transitions with three-level systems, *Phys. Rev. A* **87**, 023813 (2013).
- [56] M. Hayn and T. Brandes, Thermodynamics and superradiant phase transitions in a three-level Dicke model, *Phys. Rev. E* **95**, 012153 (2017).
- [57] J. Fan, L. Yu, G. Chen, and S. Jia, Phase-factor-dependent symmetries and quantum phases in a three-level cavity QED system, *Sci. Rep.* **6**, 25192 (2016).
- [58] W. Tian *et al.*,  $\mu$ J-level multi-cycle terahertz generation in a periodically poled Rb:KTO crystal, *Opt. Lett.* **46**, 741 (2021).
- [59] D. Zhai, E. Hérault, F. Garet, V. Pasiskevicius, F. Laurell, and J.-L. Coutaz, Two-photon-absorption enhanced terahertz generation from KTP optically pumped in the visible-to-UV range, *Opt. Express* **29**, 37683 (2021).
- [60] V. Boutou, A. Vernay, C. Félix, F. Bassignot, M. Chauvet, D. Lupinski, and B. Boulanger, Phase-matched second-harmonic generation in a flux grown KTP crystal ridge optical waveguide, *Opt. Lett.* **43**, 3770 (2018).
- [61] A. Zukauskas, G. Strömquist, V. Pasiskevicius, F. Laurell, M. Fokine, and C. Canalias, Fabrication of submicrometer quasi-phase-matched devices in KTP and RKTP, *Opt. Mater. Express* **1**, 1319 (2011).
- [62] M. Ghoohestani, A. Arab, S. J. Hashemifar, and H. Sadeghi, Ab-initio investigation of Rb substitution in KTP single crystal, *J. Appl. Phys.* **123**, 015702 (2018).
- [63] A. Marimuthu and R. N. Perumal, Investigations on structural, optical, high temperature electrical and ferroelectric properties of neodymium doped rubidium titanyl phosphate single crystal, *J. Alloys Compd.* **869**, 159284 (2021).
- [64] J. Wang, Y. Zhu, K. J. Jiang, and M. S. Zhan, Bichromatic electromagnetically induced transparency in cold rubidium atoms, *Phys. Rev. A* **68**, 063810 (2003).
- [65] C. Emary and T. Brandes, Quantum Chaos Triggered by Precursors of a Quantum Phase Transition: The Dicke Model, *Phys. Rev. Lett.* **90**, 044101 (2003).
- [66] F. Dimer, B. Estienne, A. S. Parkins, and H. J. Carmichael, Proposed realization of the Dicke-model quantum phase transition in an optical cavity QED system, *Phys. Rev. A* **75**, 013804 (2007).
- [67] H. Primakoff and T. Holstein, Many-body interactions in atomic and nuclear systems, *Phys. Rev.* **55**, 1218 (1939).
- [68] J. Radcliffe, Some properties of coherent spin states, *J. Phys. A* **4**, 313 (1971).
- [69] L. Bakemeier, A. Alvermann, and H. Fehske, Quantum phase transition in the Dicke model with critical and noncritical entanglement, *Phys. Rev. A* **85**, 043821 (2012).